Ge, Te, and Zn isotopic link between Ryugu and CI chondrites

E. Wölfer, J. Hellmann, C. Burkhardt, T. Kleine

Supplementary Information

The Supplementary Information includes:

- Extended Methods
- Tables S-1 to S-4
- Figures S-1 to S-3
- Supplementary Information References

Extended Methods

Sample Preparation and Chemical Separation of Ge, Te, and Zn

A total sample mass of ~5.4 g was collected from asteroid Ryugu and returned by the Hayabusa2 spacecraft (Tachibana *et al.*, 2022; Yada *et al.*, 2022). For this study, a subsample from sample chamber A (12.4 mg; A0220) was newly digested for combined Ge, Te, and Zn isotope analyses. To test our analytical protocol for limited sample quantities, we also digested small aliquots of Orgueil and Tarda (10–20 mg) that were taken from homogeneous bulk powders obtained from >1 g pieces (Hellmann *et al.*, 2020, 2023; Schneider *et al.*, 2023). Moreover, a ~100 mg powder aliquot of Allende was taken from a homogenous bulk powder obtained from a ~100 g piece (Hellmann *et al.*, 2020). Finally, to test for isotopic variability in CC chondrite samples on the scale of only a few mg, we carefully removed six aliquots from different domains of a large hand piece of Tagish Lake (10–15 mg, respectively).

For all samples, the (powdered) bulk rock aliquots were weighed into 60 ml Savillex PFA vials, mixed with appropriate amounts of both, a ^{70}Ge–^{73}Ge double spike (Wölfer *et al.*, 2025b), as well as a ^{123}Te–^{125}Te double spike (Hellmann *et al.*, 2020). The samples were digested on a hot-plate (120 °C, 5 days) using a (2:1) mixture of conc. HF-HNO_3. After digestion, the samples were evaporated and re-dissolved multiple times in concentrated HNO_3 at 120 °C to fume off fluorides, and ensure complete sample dissolution and sample-spike equilibration. The samples were then dried down twice in 1 M HF and finally re-dissolved in 2 ml 1 M HF in preparation for ion exchange chromatography. Fluorides that may have formed again during this step, were centrifuged and separated (see below).

In a first step, Ge was separated from the silicate matrices via a two-stage ion exchange chemistry broadly following previously established protocols (Luais, 2007, 2012; Wölfer *et al.* 2025b). The samples were loaded in 2 ml 1 M HF onto Bio-Rad columns filled with 2 ml of pre-cleaned and conditioned Bio-Rad AG 1-X8 anion exchange resin (200–400 mesh; Allende was split on three columns), and most matrix elements, including Zn (~100 %) and large parts of the Te (~80 %), were washed off by additional 13 ml 1 M HF, 2 ml H_2O, and 4 ml 0.2 M HNO_3. By contrast, Ge

together with the remaining Te (~20 %) remained on the resin and were subsequently eluted in 20 ml 0.2 M HNO_3. Germanium was then separated from Te and some remaining matrix elements using Bio-Rad columns filled with 2 ml of pre-cleaned and conditioned Bio-Rad AG 50W-X8 cation exchange resin (200–400 mesh). Sample solutions were loaded in 2 ml 0.5 M HNO_3 and Ge was directly eluted by additional 8 ml 0.5 M HNO_3, whereas Te and the remaining matrix elements remained on the resin and were subsequently washed off by 10 ml 1 M HNO_3 and 10 ml 6 M HCl. The final Ge cuts were dried down, treated with concentrated HNO_3 to destroy organic compounds from the cation resin, and then re-dissolved in 2 ml 0.5 M HNO_3 for Ge isotope measurements. The Ge yields were >90 % and the total procedural blank was <1 ng and, thus, negligible for all samples. Because the Ge double spike is added prior to sample digestion, the slightly incomplete yields are inconsequential for the Ge isotope measurements.

In preparation for the chemical separation and purification for Te and Zn, the matrix cuts from both stages of the ion exchange chemistry as well as the fluorides separated prior to sample loading were combined, evaporated to dryness, and treated with HCl to destroy the fluorides and convert the samples to chloride form. Tellurium was separated from the sample matrix using a three-stage ion exchange column chromatography (Hellmann *et al.*, 2020). The samples were dissolved in 25 ml 2 M HCl and loaded onto pre-cleaned Environmental Express ion exchange columns filled with 3 ml BioRad AG1-X8 resin (200-400 mesh). The columns were then washed sequentially with 15 ml 2 M HCl, 7 ml 11 M HCl, and 15 ml 5 M HF, where Zn was eluted and collected quantitatively in the last step. Afterwards, Te was eluted in 10 ml 1 M HNO_3, followed by several dry downs in concentrated HNO_3 and conversion to chloride form through dry downs in concentrated HCl. The Te cuts were re-dissolved in 1 ml 2 M HCl and loaded onto pre-cleaned BioRad Poly-Prep columns filled 1 ml BioRad AG1-X8 resin (200-400 mesh). In the following, the columns were washed sequentially with 5 ml 2 M HCl, 2 ml 11 M HCl, and 5 ml 5 M HF, and Te was eluted using 6 ml 0.5 M HCl. After repeated dry downs in concentrated HNO_3 and HCl, the clean-up column was repeated to reduce Sb in the Te fraction sufficiently. Finally, the Te cuts were dried down in HNO_3 and HNO_3–HCl, and then dissolved in 0.28 M HNO_3 for isotope measurements.

The Zn cuts obtained from the Te chemistry were further purified following previously established ion exchange procedures (Steller *et al.*, 2022). The samples were evaporated, converted with concentrated HCl, and loaded in 10 ml 0.8 M HCl onto precleaned Biorad columns filled with 1 ml AG1-X8 resin (200-400 mesh). Remaining matrix elements were eluted with 9 ml 0.4 M HCl and 5 ml 8 M HCl, before Zn was eluted in 7 ml 0.5 M HNO_3. This chemistry was repeated once following the same procedures, except that loading was accomplished in 1 ml 0.8 M HCl and the 8 M HCl step was omitted. The final Zn cuts were dried down in HNO_3, and then dissolved in 0.3 M HNO_3 for isotope measurements.

Isotope Measurements of Ge, Te, and Zn

The Ge isotope measurements were performed on a Thermo Scientific Neoma multicollector ICP-MS at the Max Planck Institute for Solar System Research in Göttingen, following the analytical protocol of Wölfer *et al.* (2025b). Samples were introduced using a Cetac Aridus II desolvator and a Savillex C-flow nebulizer at an uptake rate of ~70 µl/min. Using standard sampler and X skimmer cones, a signal intensity of ~10 V on ^{70}Ge was obtained for an optimally spiked ~100 ppb Ge solution. Each measurement consisted of on-peak zero measurements of 20 × 8 s, followed by 50 isotope ratio measurements of 8 s each. Isobaric interferences of Zn on ^{70}Ge and of Se on ^{74}Ge and ^{76}Ge were corrected by monitoring ^{66}Zn and ^{77}Se and using the exponential mass fractionation law. Prior to each analysis, the sample introduction system was washed using 0.28 M HNO_3 for 5 min. Processing of the measured raw data was performed off-line following the three-dimensional data reduction scheme of Siebert *et al.* (2001), as described by Wölfer *et al.* (2025b). The results are shown in the $\delta^{74/70}Ge$ notation as the permil deviation of the $^{74}Ge/^{70}Ge$ ratio of a sample from the composition of the NIST SRM 3210a Ge standard:

$$\delta^{74/70}\mathrm{Ge} = \left[\frac{(^{74}\mathrm{Ge}/^{70}\mathrm{Ge})_{\mathrm{sample}}}{(^{74}\mathrm{Ge}/^{70}\mathrm{Ge})_{\mathrm{SRM3120a}}} - 1\right] \times 1000 \qquad \text{Eq. S-1}$$

The results are reported as the mean of replicate measurements and the corresponding errors are Student-t 95 % confidence intervals (95 % CI). The accuracy and reproducibility of the Ge isotope measurements were assessed by repeated analyses of the Alfa Aesar Ge solution standard and the Allende MS-A reference material, the latter of which was processed through the full chemical separation described above and analyzed together with the other chondritic samples. The measured Ge isotopic compositions of the Alfa Aesar Ge solution standard and Allende (MS-A) are $\delta^{74/70}$Ge = –0.77 ± 0.02 (95 % CI, 2 s.d. = 0.07, N = 12) (Table S-1) and $\delta^{74/70}$Ge = 0.02 ± 0.03 (95 % CI, 2 s.d. = 0.06, N = 6), respectively, and are excellent agreement with previously reported results (Wölfer *et al.*, 2025 a,b). Along the stable isotope measurements, precise bulk Ge concentrations of the samples were determined by isotope dilution.

The Te isotope measurements were performed on a Thermo Scientific Neoma multicollector ICP-MS at the Max Planck Institute for Solar System Research in Göttingen, following the analytical protocol of Hellmann *et al.* (2020). Samples were introduced using a Cetac Aridus II desolvator and a Savillex C-flow nebulizer at an uptake rate of ~50 µl/min. Using standard sampler and X skimmer cones, total ion beam intensities of ~2× 10^{-10} A were obtained for an optimally spiked ~100 ppb Te solution. Depending on the available amount of Te, samples were measured at 30-100 ppb Te (Tagish Lake and Tarda at 30 ppb Te, Orgueil and Ryugu at 50 ppb Te, Allende at 100 ppb). Each measurement consisted of on-peak zero measurements of 25 × 4 s, followed by 50 isotope ratio measurements of 4 s each. Isobaric interferences of Xe on ^{126}Te and ^{128}Te, and of Sb on ^{123}Te were corrected by monitoring ^{129}Xe and ^{121}Sb and using the exponential mass fractionation law. Prior to each analysis, the sample introduction system was washed using 0.28 M HNO_3 for 10 min. The raw data were reduced off-line following the three-dimensional data reduction scheme of Siebert *et al.* (2001), as described by Hellmann *et al.* (2020). The results are shown in the $\delta^{128/126}$Te notation as the permil deviation of the ^{128}Ge/^{126}Ge ratio of a sample from the composition of the NIST SRM 3156 Te standard:

$$\delta^{128/126}\mathrm{Te} = \left[\frac{(^{128}\mathrm{Te}/^{126}\mathrm{Te})_{\mathrm{sample}}}{(^{128}\mathrm{Te}/^{126}\mathrm{Te}_{\mathrm{SRM3156}}} - 1\right] \times 1000 \qquad \text{Eq. S-2}$$

The results are reported as the mean of pooled solution replicates (n = 3-4) with their corresponding two standard deviation (2 s.d.). Along the stable isotope measurements, precise bulk Te concentrations of the samples were determined by isotope dilution.

The Zn isotope measurements were performed using a Thermo Scientific Neoma multicollector ICP-MS at the Max Planck Institute for Solar System Research in Göttingen, broadly following previously established protocols (Steller *et al.*, 2022). Solutions containing ~200 µg/g Zn were introduced into the mass spectrometer through an Apex 2 IR with a Savillex C-flow nebulizer at an uptake rate of ~60 µl/min. At low resolution mode and with 10^{-11} Ω feedback resistors connected to the Faraday cups, this setup resulted in a total sensitivity of ~250 V per ppm of Zn. Each measurement consisted of an on-peak zero baseline measurement of 30 × 8 s, followed by 75 isotope ratio measurements of 8 s each. Isobaric interferences of Ni on ^{64}Zn, and of Ge on ^{70}Zn were corrected by monitoring ^{61,62}Ni and ^{72,73}Ge and using the exponential mass fractionation law. Prior to each analysis, the sample introduction system was washed for 2 min using 0.3 M HNO_3. The mass-dependent Zn isotopic compositions of the samples are reported in the $\delta^{66/64}$Zn notation as the permil deviation of the ^{66}Zn/^{64}Zn ratio of a sample from the composition of the NIST SRM 683 Zn bracketing standard:

$$\delta^{66/64}\mathrm{Zn} = \left[\frac{(^{66}\mathrm{Zn}/^{64}\mathrm{Zn})_{\mathrm{sample}}}{(^{66}\mathrm{Zn}/^{64}\mathrm{Zn}_{\mathrm{SRM683}}} - 1\right] \times 1000 \qquad \text{Eq. S-3}$$

To allow for a better comparison with previous literature data, the obtained $\delta^{66/64}Zn_{SRM683}$ values are normalized to the JMC Lyon Zn standard using $\delta^{66/64}Zn_{JMC,Lyon} = \delta^{66/64}Zn_{SRM683} + 0.11$ (Chen *et al.*, 2016). The mass-dependent results are reported as the mean of pooled solution replicates (n = 6–68) and the corresponding errors are two times the standard deviation (2 s.d.). The accuracy of our mass-dependent Zn measurements was tested by analyzing the AA-ETH Zn standard and the basalt standard BIR-1a processed through our chemical procedures along with the samples. We

determined a $\delta^{66/64}Zn_{JMC,Lyon}$ = 0.28 ± 0.06 (2 s.d., N = 17) for AA-ETH Zn, and 0.27 ± 0.05 (2 s.d., N = 19) for BIR-1a (Table S-1), fully consistent with the proposed best estimate value of 0.28 ± 0.02 for AA-ETH Zn (Archer *et al.*, 2017) and 0.25 ± 0.05 for BIR-1a (Wang *et al.*, 2017).

Mass-independent Zn isotope data were obtained through mass-bias correction by internal normalization to $^{67}Zn/^{64}Zn$ = 0.08216 or $^{68}Zn/^{64}Zn$ = 0.37523 and using the exponential law, respectively. The mass-independent Zn isotope data are reported in $\mu^{i}Zn$ notation the as parts per million deviation of a sample's $^{i}Zn/^{64}Zn$ ratio from that of the NIST SRM 683 Zn bracketing standard according to:

$$\mu^{i}Zn = \left[\frac{(\,^{i}Zn/^{64}Zn)_{sample}}{(\,^{i}Zn/^{64}Zn_{SRM683}} - 1\right] \times 10^{6} \qquad \text{Eq. S-4}$$

where i = 66, 67, or 68. The external reproducibility (2 s.d.) of the bracketing NIST SRM 683 standard for a given session is on average 8 and 14 ppm for $\mu^{66}Zn$ and $\mu^{68}Zn$ (normalized to $^{67}Zn/^{64}Zn$), and 6 and 10 ppm for $\mu^{66}Zn$ and $\mu^{67}Zn$ (normalized to $^{68}Zn/^{64}Zn$), respectively. The mass-independent Zn isotope results are reported as the mean of pooled solution replicates (N = 6–27) and the corresponding errors are Student-t 95 % confidence intervals (95 % CI). The accuracy and precision of the mass-independent Zn isotope data was monitored by analyzing terrestrial standards (AA-ETH Zn [N = 17] and BIR-1a [N = 19]), which returned $\mu^{i}Zn$ signatures indistinguishable from the SRM standard at the 1-ppm-level (Table S-1).

Supplementary Tables

Table S-1 Germanium and Zn isotopic data for reference materials and terrestrial standards.

Sample	N (Ge)	$\delta^{74/70}$Ge (± 95 % CI)	N (Zn)	$\delta^{66/64}$Zn (± 2 s.d.)	μ^{66}Zn (± 95 % CI)	μ^{68}Zn (± 95 % CI)	μ^{66}Zn (± 95 % CI)	μ^{68}Zn (± 95 % CI)
					^{67}Zn/^{64}Zn int. norm.		^{68}Zn/^{64}Zn int. norm.	
Ge Alfa Aesar	12	−0.77 ± 0.02						
AA-ETH Zn			17	0.28 ± 0.06	0 ± 2	0 ± 2	0 ± 1	0 ± 2
BIR-1a			19	0.27 ± 0.05	0 ± 2	1 ± 3	−1 ± 1	−1 ± 2

Table S-2 Germanium concentration and isotopic data for chondrite samples investigated in this study and comparison to literature data.

Sample	Ge (µg/g)	$\delta^{74/70}$Ge (± 95 % CI)	References
Orgueil	34.6	1.00 ± 0.04	(1)
Orgueil (this study)	33.9	1.01 ± 0.03	
Tagish Lake	27.5	0.71 ± 0.04	(1)
Tagish Lake (this study)	25.6	0.67 ± 0.03	
Tagish Lake (this study)	25.2	0.65 ± 0.03	
Tagish Lake (this study)	25.1	0.66 ± 0.04	
Tagish Lake (this study)	25.5	0.67 ± 0.02	
Tagish Lake (this study)	26.2	0.71 ± 0.03	
Tagish Lake (this study)	25.5	0.72 ± 0.02	
Tarda	24.1	0.79 ± 0.04	(1)
Tarda (this study)	24.4	0.73 ± 0.03	
Allende	16.8	-0.02 ± 0.05	(1)
Allende (this study)	17.2	0.02 ± 0.03	

References: (1) Wölfer *et al.* (2025a).

Table S-3 Tellurium concentration and isotopic data for chondrite samples investigated in this study and comparison to literature data.

Sample	Te (µg/g)	$\delta^{128/126}$Te (± 2 s.d.)	References
Orgueil	2.250	0.16 ± 0.01	(1)
Orgueil	2.190	0.20 ± 0.07	(2)
Lit. Av.	2.220	0.18 ± 0.06	
Orgueil (this study)	2.269	0.15 ± 0.02	
Tagish Lake	1.669	0.11 ± 0.01	(1)
Tagish Lake (this study)	1.729	0.13 ± 0.03	
Tagish Lake (this study)	1.764	0.12 ± 0.03	
Tagish Lake (this study)	1.556	0.12 ± 0.06	
Tagish Lake (this study)	1.647	0.10 ± 0.01	
Tagish Lake (this study)	1.756	0.12 ± 0.05	
Tagish Lake (this study)	1.691	0.11 ± 0.03	
Tarda	1.563	0.08 ± 0.01	(3)
Tarda (this study)	1.622	0.07 ± 0.07	
Allende	0.948	0.02 ± 0.02	(1)
Allende	0.939	0.02 ± 0.01	(1)
Allende	0.899	0.01 ± 0.04	(2)
Allende	0.833	0.00 ± 0.01	(2)
Lit. Av.	0.905	0.01 ± 0.02	
Allende (this study)	0.954	0.02 ± 0.02	

References: (1) Hellmann *et al.* (2020); (2) Morton *et al.* (2024); (3) Hellmann *et al.* (2023).

Table S-4 Zinc concentration and isotopic data for chondrite samples investigated in this study and comparison to literature data.

Sample	Zn (µg/g)	$\delta^{66/64}$Zn (± 2 s.d.)	References
Ryugu	361	0.43 ± 0.05	(4)
Ryugu (this study)	348	0.51 ± 0.12	
Orgueil	307	0.46 ± 0.05	(1)
Orgueil	307	0.52 ± 0.05	(1)
Orgueil	307	0.42 ± 0.09	(2)
Orgueil	303	0.45 ± 0.09	(2)
Orgueil	303	0.43 ± 0.09	(2)
Orgueil	311	0.43 ± 0.09	(2)
Orgueil	291	0.51 ± 0.09	(2)
Orgueil	272	0.45 ± 0.09	(2)
Orgueil	296	0.42 ± 0.04	(3)
Orgueil	288	0.52 ± 0.08	(4)
Lit. Av.	**299**	**0.46 ± 0.08**	
Orgueil (this study)	318	0.51 ± 0.08	
Orgueil (this study)	298	0.53 ± 0.11	
Tagish Lake	214	0.43 ± 0.05	(1)
Tagish Lake	207	0.47 ± 0.05	(1)
Tagish Lake	209	0.41 ± 0.05	(1)
Tagish Lake	209	0.47 ± 0.05	(1)
Tagish Lake	204	0.42 ± 0.06	(4)
Lit. Av.	**209**	**0.44 ± 0.06**	
Tagish Lake (this study)	196	0.51 ± 0.08	
Tagish Lake (this study)	202	0.63 ± 0.05	
Tagish Lake (this study)	188	0.52 ± 0.04	
Tagish Lake (this study)	187	0.57 ± 0.06	
Tagish Lake (this study)	197	0.53 ± 0.09	
Tagish Lake (this study)	188	0.48 ± 0.03	
Tarda	201	0.46 ± 0.07	(4)
Tarda (this study)	194	0.54 ± 0.05	
Tarda (this study)	205	0.46 ± 0.06	
Jbilet Winselwan	181	0.33 ± 0.04	(3)
Jbilet Winselwan (this study)	183	0.41 ± 0.08	
Allende	117	0.37 ± 0.05	(1)
Allende		0.32 ± 0.05	(1)
Allende	112	0.27 ± 0.04	(5)
Allende	108	0.30 ± 0.02	(5)
Allende		0.26 ± 0.12	(6)
Allende	99	0.12 ± 0.05	(3)
Allende	100	0.23 ± 0.05	(3)
Allende	110	0.22 ± 0.07	(4)
Allende	121	0.24 ± 0.06	(4)
Lit. Av.	**110**	**0.26 ± 0.14**	
Allende (this study)	111	0.31 ± 0.07	
Allende (this study)	108	0.27 ± 0.08	
Vigarano	116	0.28 ± 0.05	(1)
Vigarano (this study)	104	0.17 ± 0.05	

References: (1) Luck *et al.* (2005); (2) Barrat *et al.* (2012); (3) Morton *et al.* (2024); (4) Paquet *et al.* (2023); (5) Pringle *et al.* (2017); (6) Makishima and Nakamura (2013).

Supplementary Figures

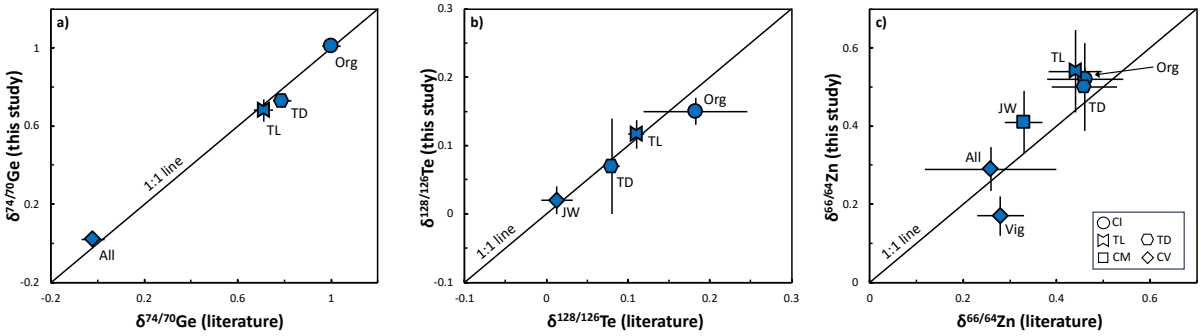

Figure S-1 Diagrams of the **(a)** Ge, **(b)** Te, and **(c)** Zn mass-dependent isotopic compositions of carbonaceous chondrites reported in the literature in comparison to the results of this study. Each point represents the average composition of a given sample. Stated uncertainties represent two times the standard deviation (2 s.d) in case of Te and Zn, and 95 % confidence intervals (95 % CI) in case of Ge. Individual literature data are reported in Tables S-2 to S-4.

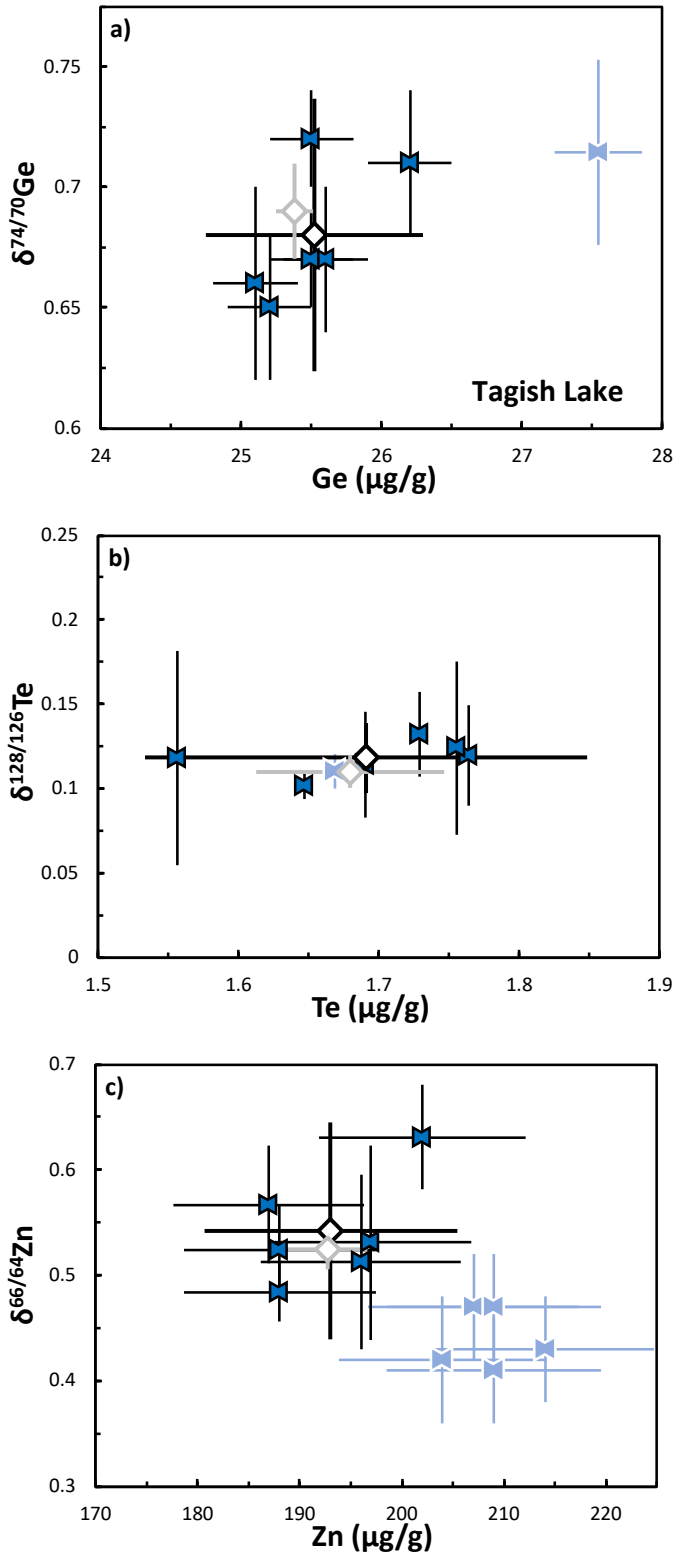

Figure S-2 Diagrams of **(a)** Ge concentrations vs. $\delta^{74/70}$Ge variations, **(b)** Te concentrations vs. $\delta^{128/126}$Te variations, and **(c)** Zn concentrations vs. $\delta^{66/64}$Zn variations of Tagish Lake (data from this study in dark blue [average (2 s.d.) in black; weighted mean in grey]; literature data in light blue). Literature data for Ge is from Wölfer *et al.* (2025a); data for Te is from Hellmann *et al.* (2020).

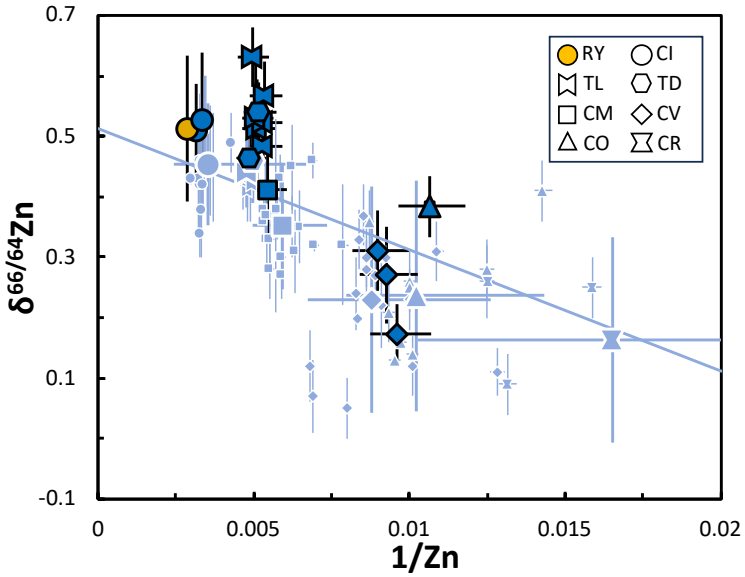

Figure S-3 Diagram of 1/Zn vs. $\delta^{66/64}$Ge variations of carbonaceous chondrites (data from this study in dark blue; literature data in light blue [small symbols represent individual samples; large symbols represent the group averages]) and Ryugu sample A0220 (orange circle). Literature data are from Luck *et al.* (2005), Barrat *et al.* (2012), Pringle *et al.* (2017), Mahan *et al.* (2018), Paquet *et al.* (2023), and Morton *et al.* (2024). All Zn isotope data are shown relative to the JMC Lyon reference standard. The blue line represents the weighted regression calculated using IsoplotR and is based on the group averages compiled from the literature.

Supplementary Information References

Archer, C., Andersen, M.B., Cloquet, C., Conway, T.M., Dong, S. *et al.* (2017) Inter-calibration of a proposed new primary reference standard AA-ETH Zn for zinc isotopic analysis. *Journal of Analytical Atomic Spectrometry* 32, 415–419. https://doi.org/10.1039/C6JA00282J

Barrat, J.A., Zanda, B., Moynier, F., Bollinger, C., Liorzou, C., Bayon, G. (2012) Geochemistry of CI chondrites: Major and trace elements, and Cu and Zn Isotopes. *Geochimica et Cosmochimica Acta* 83, 79–92. https://doi.org/10.1016/j.gca.2011.12.011

Chen, S., Liu, Y., Hu, J., Zhang, Z., Hou, Z., Huang, F., Yu, H. (2016) Zinc Isotopic Compositions of NIST SRM 683 and Whole-Rock Reference Materials. *Geostandards and Geoanalytical Research* 40, 417–432. https://doi.org/10.1111/j.1751-908X.2015.00377.x

Hellmann, J.L., Hopp, T., Burkhardt, C., Kleine, T. (2020) Origin of volatile element depletion among carbonaceous chondrites. *Earth and Planetary Science Letters* 549, 116508. https://doi.org/10.1016/j.epsl.2020.116508

Hellmann, J.L., Schneider, J.M., Wölfer, E., Drążkowska, J., Jansen, C.A., Hopp, T., Burkhardt, C., Kleine, T. (2023) Origin of Isotopic Diversity among Carbonaceous Chondrites. *The Astrophysical Journal Letters* 946, L34. https://doi.org/10.3847/2041-8213/acc102

Luais, B. (2007) Isotopic fractionation of germanium in iron meteorites: Significance for nebular condensation, core formation and impact processes. *Earth and Planetary Science Letters* 262, 21–36. https://doi.org/10.1016/j.epsl.2007.06.031

Luais, B. (2012) Germanium chemistry and MC-ICPMS isotopic measurements of Fe–Ni, Zn alloys and silicate matrices: Insights into deep Earth processes. *Chemical Geology* 334, 295–311. https://doi.org/10.1016/j.chemgeo.2012.10.017

Luck, J.-M., Othman, D.B., Albarède, F. (2005) Zn and Cu isotopic variations in chondrites and iron meteorites: Early solar nebula reservoirs and parent-body processes. *Geochimica et Cosmochimica Acta* 69, 5351–5363. https://doi.org/10.1016/j.gca.2005.06.018

Mahan, B., Moynier, F., Beck, P., Pringle, E.A., Siebert, J. (2018) A history of violence: Insights into post-accretionary heating in carbonaceous chondrites from volatile element abundances, Zn isotopes and water contents. *Geochimica et Cosmochimica Acta* 220, 19–35. https://doi.org/10.1016/j.gca.2017.09.027

Makishima, A., Nakamura, E. (2013) Low-blank chemistry for Zn stable isotope ratio determination using extraction chromatographic resin and double spike-multiple collector-ICP-MS. *Journal of Analytical Atomic Spectrometry* 28, 127–133. https://doi.org/10.1039/C2JA30271C

Morton, E.M., Pickard, H., Wombacher, F., Huang, Y., Palk, E., Martins, R., Kuthning, S., Schönbächler, M., Rehkämper, M. (2024) Volatile Element Depletion of Carbonaceous Chondrites—Insights from Mass-dependent Zinc, Cadmium, and Tellurium Isotope Variations. *The Astrophysical Journal* 977, 53. https://doi.org/10.3847/1538-4357/ad87ed

Paquet, M., Moynier, F., Yokoyama, T., Dai, W., Hu, Y. *et al.* (2023) Contribution of Ryugu-like material to Earth's volatile inventory by Cu and Zn isotopic analysis. *Nature Astronomy* 7, 182–189. https://doi.org/10.1038/s41550-022-01846-1

Pringle, E.A., Moynier, F., Beck, P., Paniello, R., Hezel, D.C. (2017) The origin of volatile element depletion in early solar system material: Clues from Zn isotopes in chondrules. *Earth and Planetary Science Letters* 468, 62–71. https://doi.org/10.1016/j.epsl.2017.04.002

Schneider, J.M., Burkhardt, C., Kleine, T. (2023) Distribution of *s*-, *r*-, and *p*-process Nuclides in the Early Solar System Inferred from Sr Isotope Anomalies in Meteorites. *The Astrophysical Journal Letters* 952, L25. https://doi.org/10.3847/2041-8213/ace187

Siebert, C., Nägler, T.F., Kramers, J.D. (2001) Determination of molybdenum isotope fractionation by double-spike multicollector inductively coupled plasma mass spectrometry. *Geochemistry, Geophysics, Geosystems* 2, 2000GC000124. https://doi.org/10.1029/2000GC000124

Steller, T., Burkhardt, C., Yang, C., Kleine, T. (2022) Nucleosynthetic zinc isotope anomalies reveal a dual origin of terrestrial volatiles. *Icarus* 386, 115171. https://doi.org/10.1016/j.icarus.2022.115171

Tachibana, S., Sawada, H., Okazaki, R., Takano, Y., Sakamoto, K. *et al.* (2022) Pebbles and sand on asteroid (162173) Ryugu: In situ observation and particles returned to Earth. *Science* 375, 1011–1016. https://doi.org/10.1126/science.abj8624

Wang, Z.-Z., Liu, S.-A., Liu, J., Huang, J., Xiao, Y., Chu, Z.-Y., Zhao, X.-M., Tang, L. (2017) Zinc isotope fractionation during mantle melting and constraints on the Zn isotope composition of Earth's upper mantle. *Geochimica et Cosmochimica Acta* 198, 151–167. https://doi.org/10.1016/j.gca.2016.11.014

Wölfer, E., Burkhardt, C., Nimmo, F., Kleine, T. (2025a) Origin of moderately volatile elements in Earth inferred from mass-dependent Ge isotope variations among chondrites. *Earth and Planetary Science Letters* 663, 119435. https://doi.org/10.1016/j.epsl.2025.119435

Wölfer, E., Burkhardt, C., Kleine, T. (2025b) Germanium stable isotope measurements by double-spike MC-ICPMS. *Journal of Analytical Atomic Spectrometry* 40, 1023–1036. https://doi.org/10.1039/D4JA00359D

Yada, T., Abe, M., Okada, T., Nakato, A., Yogata, K. *et al.* (2022) Preliminary analysis of the Hayabusa2 samples returned from C-type asteroid Ryugu. *Nature Astronomy* 6, 214–220. https://doi.org/10.1038/s41550-021-01550-6